



## Hypoxia inducible factor-1 $\alpha$ facilitates transmissible gastroenteritis virus replication by inhibiting type I and type III interferon production

Yunhang Zhang<sup>a,b,c</sup>, Xue Rui<sup>a,c,e</sup>, Yang Li<sup>a</sup>, Yue Zhang<sup>a</sup>, Yifei Cai<sup>a,c,d</sup>, Chen Tan<sup>a,b,c</sup>,  
Ning Yang<sup>a,b,c</sup>, Yuanyuan Liu<sup>a,c,e</sup>, Yuguang Fu<sup>a</sup>, Guangliang Liu<sup>a,c,e,\*</sup>

<sup>a</sup> State Key Laboratory for Animal Disease Control and Prevention, College of Veterinary Medicine, Lanzhou University, Lanzhou Veterinary Research Institute, Chinese Academy of Agricultural Sciences, China

<sup>b</sup> Molecular and Cellular Epigenetics (GIGA) and Molecular Biology (TERRA), University of Liege, Belgium

<sup>c</sup> Hainan Key Laboratory of Tropical Animal Breeding and Infectious Disease Research, Institute of Animal Husbandry and Veterinary Medicine, Hainan Academy of Agricultural Sciences, China

<sup>d</sup> Nutritional Biology, Wageningen University and Research, Wageningen, the Netherlands

<sup>e</sup> College of Veterinary Medicine, Xinjiang Agricultural University, China

### ARTICLE INFO

#### Keywords:

TGEV  
HIF-1 $\alpha$   
Intestinal organoid monolayer  
Type I and type III IFN production  
*In vivo*

### ABSTRACT

Transmissible gastroenteritis virus (TGEV) is characterized by watery diarrhea, vomiting, and dehydration and is associated with high mortality especially in newborn piglets, causing significant economic losses to the global pig industry. Hypoxia inducible factor-1 $\alpha$  (HIF-1 $\alpha$ ) has been identified as a key regulator of TGEV-induced inflammation, but understanding of the effect of HIF-1 $\alpha$  on TGEV infection remains limited. This study found that TGEV infection was associated with a marked increase in HIF-1 $\alpha$  expression in ST cells and an intestinal organoid epithelial monolayer. Furthermore, HIF-1 $\alpha$  was shown to facilitate TGEV infection by targeting viral replication, which was achieved by restraining type I and type III interferon (IFN) production. *In vivo* experiments in piglets demonstrated that the HIF-1 $\alpha$  inhibitor BAY87-2243 significantly reduced HIF-1 $\alpha$  expression and inhibited TGEV replication and pathogenesis by activating IFN production. In summary, we unveiled that HIF-1 $\alpha$  facilitates TGEV replication by restraining type I and type III IFN production *in vitro*, *ex vivo*, and *in vivo*. The findings from this study suggest that HIF-1 $\alpha$  could be a novel antiviral target and candidate drug against TGEV infection.

### 1. Introduction

Transmissible gastroenteritis virus (TGEV), a member of the genus *Alphacoronavirus* (family *Coronaviridae*, order *Nidovirales*), is a single-stranded, positive-sense RNA virus (Liu and Wang, 2021). TGEV infection causes acute watery diarrhea, vomiting, dehydration, and anorexia and is associated with high morbidity and mortality, particularly in nursing piglets (Chen et al., 2023). The innate immune response defends the host against invading pathogens. Upon TGEV infection, pattern recognition receptors (PRRs) such as toll-like receptors (TLRs) and retinoic acid inducible gene-I (RIG-I)-like receptors (RLRs) are activated through their recognition of pathogen-associated molecular patterns (PAMPs) released by TGEV. PRR activation induces downstream signaling cascades that recruit and activate TBK1/IKK $\epsilon$  and cause the nuclear translocation of IRF3/7 and P65, resulting in the production of interferons (IFNs) and inflammatory cytokines (Zhang et al., 2022).

Type I and type III IFNs interact with their receptors and induce the production of hundreds of IFN-stimulated genes (ISGs) through JAK/STAT signaling (Schneider et al., 2014).

Type I and type III IFNs and ISGs play a critical role in the defense against virus infection (Zhang et al., 2022; Zhang et al., 2019). For example, IFN- $\beta$  and IFN- $\lambda$ 1/3 have a strong antiviral effect on coronavirus infections, especially among pigs (Ding et al., 2018; Park and Iwasaki, 2020; Zhang et al., 2018). Several ISGs are also reported to restrict infections with coronaviruses. For example, oligoadenylate synthetase-like (OASL) can significantly inhibit porcine epidemic diarrhea virus (PEDV) and TGEV infection (Song et al., 2022). In addition, IFN-stimulated gene 15 (ISG15) conjugation is essential for antiviral IFN responses against coronavirus infections (Liu et al., 2021). Meanwhile, coronaviruses have evolved to subvert host immunity by targeting key proteins participating in the IFN response (Bouhaddou et al., 2023). PEDV non-structure protein 1 (nsp1) inhibits type III IFN production by

\* Correspondence to: 1 XuJiaPing, YanChangBu, ChengGuan District, Lanzhou, Gansu 730046, China.

E-mail address: [LiuGuangliang01@caas.cn](mailto:LiuGuangliang01@caas.cn) (G. Liu).

<https://doi.org/10.1016/j.vetmic.2024.110055>

Received 29 October 2023; Received in revised form 9 March 2024; Accepted 13 March 2024

Available online 16 March 2024

0378-1135/© 2024 Elsevier B.V. All rights reserved.

blocking the nuclear translocation of IRF1 and reducing the number of peroxisomes (Zhang et al., 2018). In addition, SARS-CoV-2 PLpro can cleave ISG15 from IRF3 and attenuate type I IFN responses (Shin et al., 2020). Thus, positive regulation of type I and type III IFNs is one mechanism for improving the host antiviral response against invading viruses.

Hypoxia inducible factor-1 $\alpha$  (HIF-1 $\alpha$ ) is a major transcriptional activator that allows cells to adapt to hypoxia and acts as a key regulator of the innate immune response (Koyasu et al., 2018). Peng et al. reported that hypoxia-induced HIF-1 $\alpha$  directly represses IRF5 and IRF3 transcription and negatively regulates type I IFN signaling, inducing inflammatory cytokine production by monocytes (Peng et al., 2021). In addition, HIF-1 $\alpha$  has been shown to regulate various viral infections, including SARS-CoV-2, vesicular stomatitis virus (VSV), herpes simplex virus type 1 (HSV-1) (Tian et al., 2021), and H1N1 virus (Meng et al., 2023). Furthermore, porcine reproductive and respiratory syndrome virus (PRRSV) nsp1 $\beta$  stabilizes HIF-1 $\alpha$  to enhance viral replication (Pang et al., 2022). However, the effect of HIF-1 $\alpha$  on TGEV infection is unknown and warrants further investigation, with the aim of providing a reliable target against TGEV infection.

This study found that TGEV infection was associated with increased HIF-1 $\alpha$  expression *in vitro* and *ex vivo*. HIF-1 $\alpha$  promoted TGEV infection by targeting viral replication in ST cells and an intestinal organoid monolayer. The effect of HIF-1 $\alpha$  on TGEV infection was primarily dependent on the downregulation of type I and type III IFN production. *In vivo* experiments in pigs highlighted the same molecular mechanism by which HIF-1 $\alpha$  promotes TGEV replication. In summary, HIF-1 $\alpha$  was shown to facilitate TGEV replication by restraining type I and type III IFN production.

## 2. Materials and methods

### 2.1. Cell culture, virus, and animals

ST cells and Vero-APN cells were maintained in Dulbecco's Modified Eagle's Medium (DMEM) (Sigma-Aldrich, USA, D6429) with 10% fetal bovine serum (Invigentech, Brazil, A6901). The cells were incubated at 37 °C in a humidified incubator with 5% CO<sub>2</sub>. The TGEV Miller strain was maintained at a titer of 10<sup>7.25</sup> TCID<sub>50</sub>/mL, where TCID<sub>50</sub> is the 50% tissue culture infectious dose. Porcine intestines used for crypt isolation were obtained from the Luoniushan Co., Ltd slaughterhouse in Hainan Province, China.

### 2.2. Porcine intestinal 3D organoid culture

Porcine ileum crypts were isolated from pigs and cultured in Matrigel (Corning, USA, 356231) and Organoid Growth Medium (OGM) (Stem Cell, Canada, 06010) containing 10  $\mu$ M of the ATP-competitive inhibitor of Rho-associated kinases (Y-27632; CST, USA, 72302) as previously described (Li et al., 2020).

### 2.3. Establishment of the intestinal organoid monolayer

After 5 days of culture, 3D ileum organoids were collected using ice-cold DMEM and centrifuged at 250 g for 5 min. The organoid pellet without Matrigel was dissociated into single cells or small fragments at 37 °C using TryPLE Express (Gibco, USA, 12605-010) by repeated pipetting to release the organoids after two 5 min intervals. Signal cells or small fragments were resuspended in OGM containing 10  $\mu$ M Y-27632 and seeded into a 48-well plate with 1.5% Matrigel. The monolayer reached confluency after 3 days of culture and was used for follow-up experiments (Yang et al., 2022a).

### 2.4. Virus infection in the intestinal organoid monolayer

The organoid monolayer cultured for 3 days was inoculated with the

**Table 1**  
Antibodies used in this study.

Antibody	Type	Supplier	Product Number
HIF-1 $\alpha$	Rabbit	Proteintech	20960-1-AP
GAPDH	Rabbit	Proteintech	10494-1-AP

**Table 2**  
Primers used for real-time qPCR.

Names	Primer or probe	Sequence (5'-3')
TGEV N	Forward	TGCCATGAACAAACCAAC GGCACCTTACCATCGAAT
	Reverse	HEX-TAGCACACGACTACCAAGC-BHQ1a
GRP78	Forward	TCTACTCGCATCCCAAAG
	Reverse	CTCCCACGGTTTCAATAC
ATP4	Forward	TGGAGCAGAACAAGACAGC
	Reverse	CTTTACATTCGCCAGTGAG
LC3B	Forward	CCGAACCTCGAACAGAGAG
	Reverse	AGGCTTGGTTAGCATTGAGC
ATG7	Forward	AGATTGCCTGGTGGGTGGT
	Reverse	GGGTGATGTGGAGGAGTTG
Caspase3	Forward	TGGGATTGAGACGGACAGTG
	Reverse	CGCTGCACAAAGTGACTGGA
FasL	Forward	GGGTTCCTCTGTCACCTGGTA
	Reverse	TCAGCATGTTTCCGTTTGCC
IFN- $\beta$	Forward	CCACCACAGCTCTTCCATGA
	Reverse	TGAGGAGTCCCAGGCAACT
IFN- $\lambda$ 1	Forward	CCACGTCGAACCTCAGGCTT
	Reverse	ATGTGCAAGTCTCCACTGGT
IFN- $\lambda$ 3	Forward	GCCAAGGATGCCTTTGAAGAG
	Reverse	CAGGACGCTGAGGTCAGG
OASL	Forward	TCCCTGGGAAGAATGTGCAG
	Reverse	CCCTGGCAAGAGCATAGTGT
HIF-1 $\alpha$	Forward	GGCGGACACGACAAGAAAA
	Reverse	GTGGCAACTGATGAGCAAGC
ISG15	Forward	GGTGAGGAACGACAAGGGTC
	Reverse	GGCTTGAGGTCATACTCCCC
ISG56	Forward	AAATGAATGAAGCCCTGGAGTATT
	Reverse	AGGGATCAAGTCCCACAGATTTT

TGEV Miller strain (multiplicity of infection [MOI] = 1) for 2 h at 37 °C. Residual viruses were removed by washing with phosphate-buffered saline (PBS). The organoid monolayer was then cultured with OGM (with 10  $\mu$ M Y-27632) for the indicated times (Yang et al., 2022a).

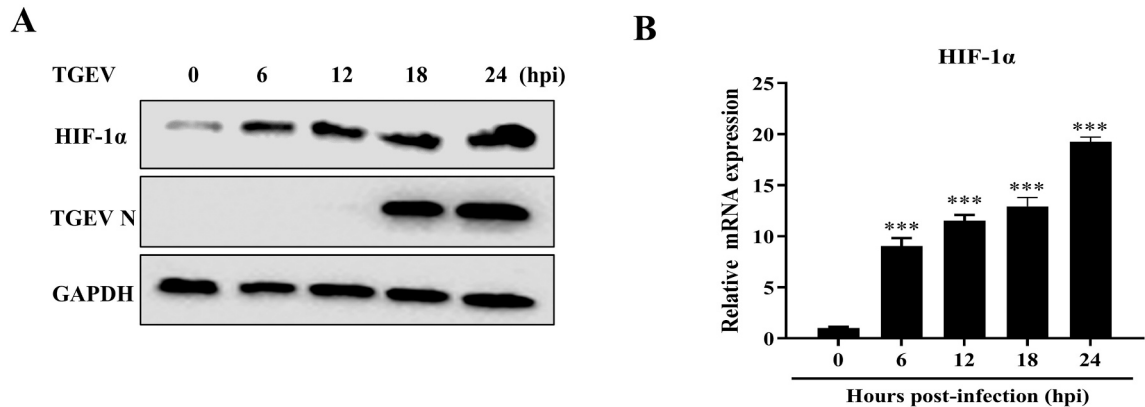
### 2.5. Histopathological and immunofluorescence analysis

The small intestine was collected, fixed for 24 h in 10% formalin, dehydrated according to the standard protocol, embedded in paraffin, and stained with hematoxylin and eosin using standard procedures (Yang et al., 2022b). For immunofluorescence analysis, ST cells or different segments of the small intestine were fixed with 4% paraformaldehyde for 20 min and permeabilized with 0.1% Triton X-100 (Beyotime, China, ST797) for 20 min at 37 °C. The samples were blocked with 5% bovine serum albumin (Biofroxx, Germany, 4240GR100) for 1 h and labeled with primary antibodies overnight at 4 °C. After rinsing, the samples were incubated with secondary antibodies for 1 h at room temperature. The nuclei were then stained with 4', 6'-diamidino-2-phenylindole (DAPI; Beyotime, China, C1006). After washing, the samples were visualized using confocal laser-scanning microscopy (Zeiss LSM 900, Germany).

### 2.6. Western blotting

Proteins were separated by sodium dodecyl sulfate-polyacrylamide gel electrophoresis (SDS-PAGE) and transferred onto a polyvinylidene fluoride (PVDF) membrane (GE, USA, 10600023). The membranes were blocked in 5% nonfat milk at room temperature for 2 h and incubated

## ST Cells



## Intestinal organoid monolayer

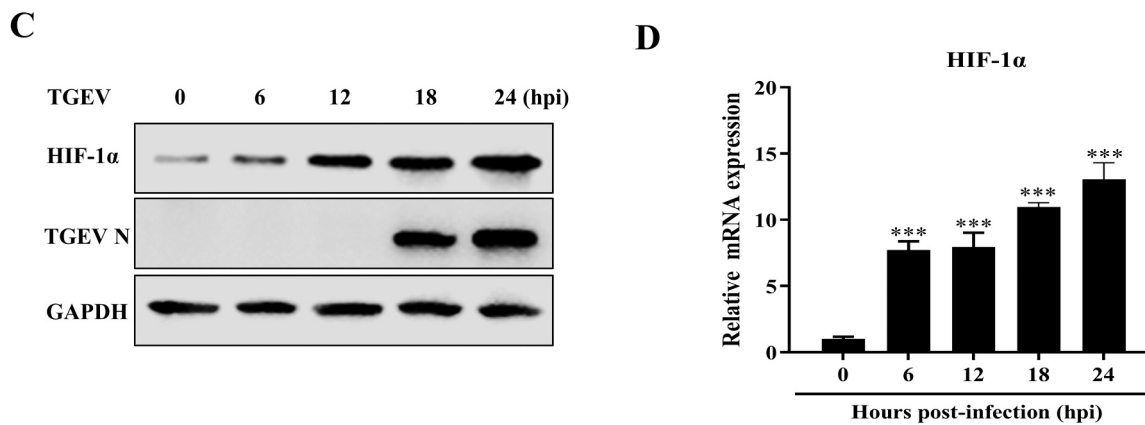


**Fig. 1.** TGEV infection promotes HIF-1 $\alpha$  expression *in vitro* and *ex vivo*. (A, B) ST cells were infected with TGEV at a multiplicity of infection (MOI) of 1 for 0, 6, 12, 18, and 24 h, and HIF-1 $\alpha$  expression was measured by western blotting (A) and RT-qPCR (B). (C, D) The intestinal organoid monolayer was infected with TGEV at an MOI of 1 for the indicated time points and HIF-1 $\alpha$  expression was measured by western blotting (C) and RT-qPCR (D). Results are presented as the mean  $\pm$  standard deviation of data from three independent experiments. \*\*\*,  $P \leq 0.001$ , determined by two-tailed Student's *t*-test.

overnight with the primary antibodies specified in Table 1. The membranes were then incubated with a secondary antibody for 1 h at room temperature. Finally, proteins were visualized using WesternBright ECL (Advansta, USA, K-12045-D50) (Zhang et al., 2021).

### 2.7. RNA extraction, real-time quantitative PCR (RT-qPCR), and enzyme-linked immunosorbent assay (ELISA)

Total RNA was extracted using RNAiso reagent (TaKaRa, Japan, 9109) and reverse transcribed into cDNA using HiScript Q RT SuperMix for qPCR (Vazyme, China, R223-01), according to the manufacturer's instructions. The TGEV virus copy number was detected using a TaqMan probe-based RT-qPCR developed previously (Huang et al., 2019). Relative qPCR was performed using the ChamQ SYBR qPCR master mix (Vazyme, China, Q311-02) and calculated with the  $2^{-\Delta\Delta CT}$  method. The primers and probe used in this study are listed in Table 2. For the ELISA assay, IFN- $\beta$  in the supernatant of TGEV-infected ST cells and the intestinal content of piglets sacrificed at 24 h post-infection (hpi) was detected using a commercial kit according to the manufacturer's instructions (NEWA, China, SY-P00306).

### 2.8. Animal experiments

Neonatal pigs spontaneously delivered from sows were confirmed negative for TGEV by RT-qPCR and ELISA. The piglets were randomly

separated into three groups: mock (3), TGEV (3), and TGEV-BAY87 (3). In the TGEV group, the piglets were orally infected with  $1.245 \times 10^8$  plaque-forming units (PFU) of TGEV Miller strain. In the TGEV-BAY87 group, piglets were orally infected with  $1.245 \times 10^8$  PFU of TGEV Miller strain and treated with BAY87 (10 mg/kg). All piglets were euthanized at 24 hpi, and the intestinal tissues were collected for RT-qPCR, western blotting, and pathological examination.

### 2.9. Ethics statement

All animals were handled in strict accordance with good animal practice according to the Animal Ethics Procedures and Guidelines of the People's Republic of China. The study was approved by The Animal Administration and Ethics Committee of Lanzhou Veterinary Research Institute, Chinese Academy of Agricultural Sciences (Permit No. LVRIAEC-2020-030).

### 2.10. Statistical analysis

All data were analyzed using GraphPad Prism 8.0 software (GraphPad, La Jolla, CA, USA) by one-/two-way analysis of variance. Results are presented as the mean  $\pm$  standard deviation of data from three independent experiments. \*,  $P \leq 0.05$ ; \*\*,  $P \leq 0.01$ ; \*\*\*,  $P \leq 0.001$ ; ns, not significant, as determined by two-tailed Student's *t*-test. Each experiment was performed with three biological replicates.

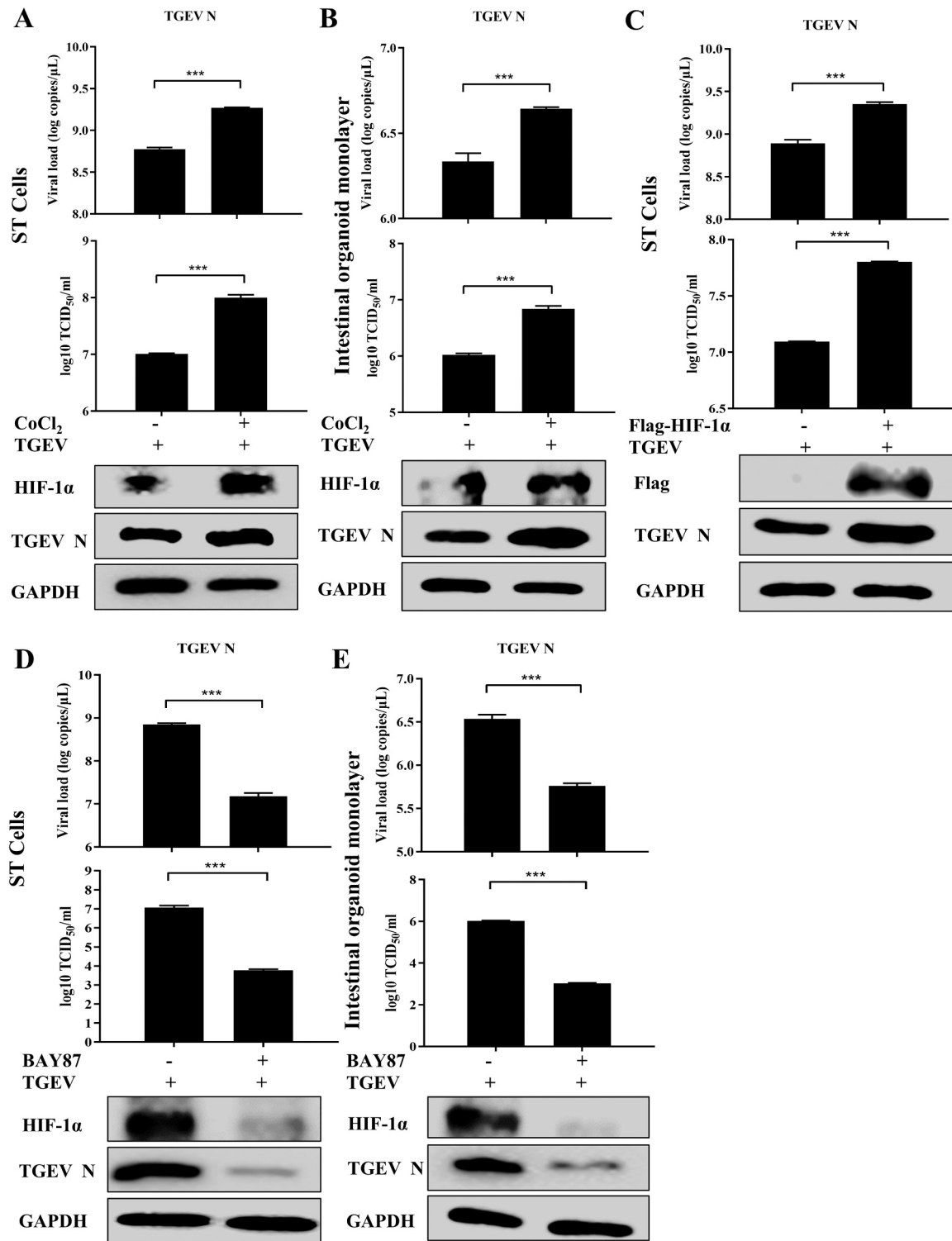


**Fig. 2.** HIF-1 $\alpha$  promotes TGEV infection in ST cells and the intestinal organoid monolayer. (A, B) ST cells (A) or the intestinal organoid monolayer (B) were pretreated with CoCl<sub>2</sub> (25  $\mu$ M) for 1 h, infected with TGEV (multiplicity of infection [MOI]=1) for 1 h, and treated again with CoCl<sub>2</sub> at 37 °C for 19 h. Cell samples were collected and examined by RT-qPCR, 50% tissue culture infectious dose (TCID<sub>50</sub>) assay, and western blotting. (C) ST cells were transfected with Flag-HIF-1 $\alpha$  for 24 h and infected with TGEV (MOI=1) for 20 h. HIF-1 $\alpha$  was detected by RT-qPCR, TCID<sub>50</sub> assay, and western blotting. (D, E) ST cells (D) or the intestinal organoid monolayer (E) were pretreated with BAY87 (10  $\mu$ M) for 1 h and then infected with TGEV (MOI=1) for 20 h. Cell samples were collected and examined by RT-qPCR, TCID<sub>50</sub> assay, and western blotting. Results are presented as the mean  $\pm$  standard deviation of data from three independent experiments \*\*\*,  $P \leq 0.001$ , determined by two-tailed Student's *t*-test.

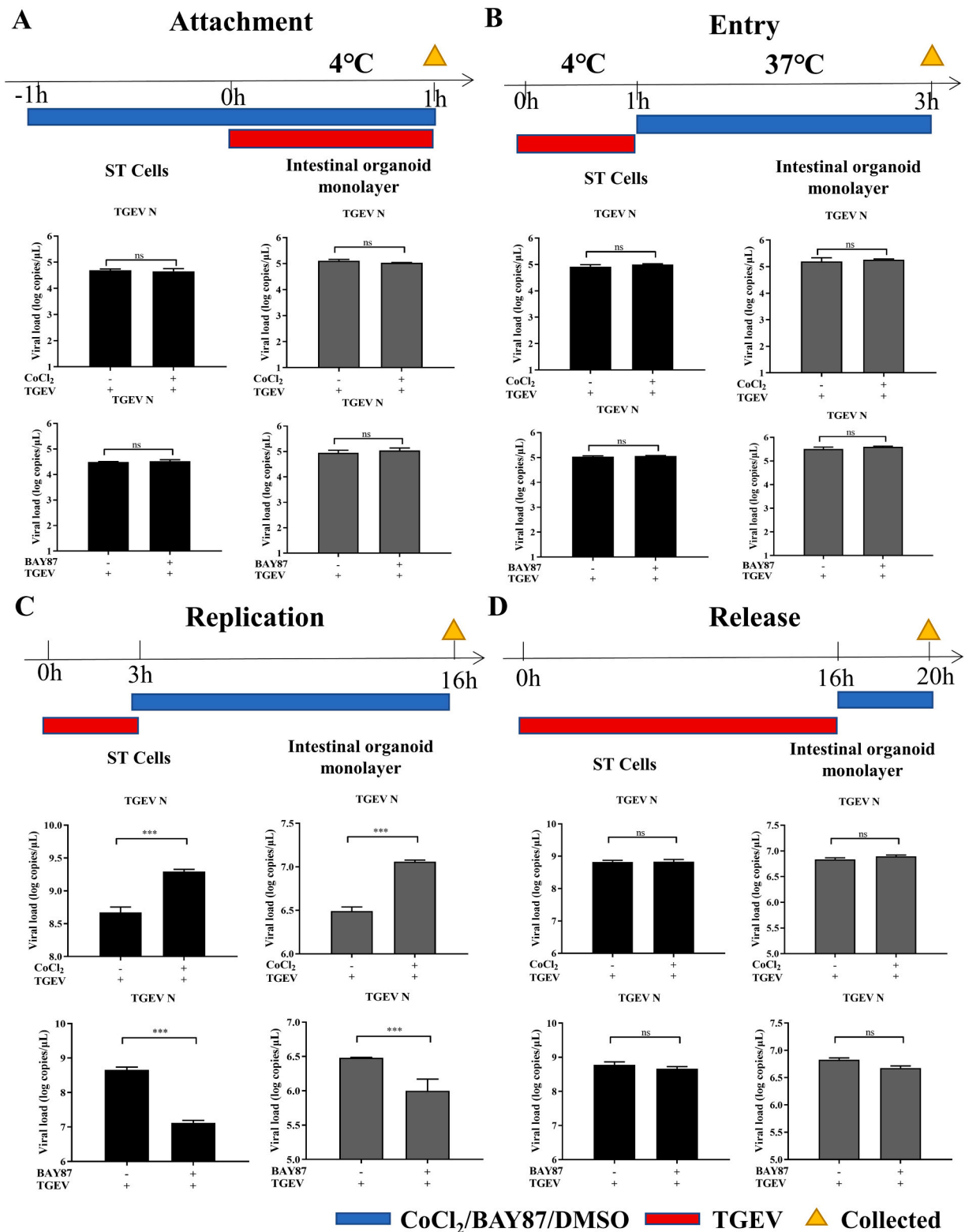


**Fig. 3.** HIF-1 $\alpha$  enhances TGEV infection by targeting viral replication. (A) Adsorption assay. ST cells (left) or the intestinal organoid monolayer (right) were pretreated with CoCl<sub>2</sub> (25  $\mu$ M), BAY87 (10  $\mu$ M), or DMSO for 1 h at 37  $^{\circ}$ C, and the media were replaced by a mixture of CoCl<sub>2</sub> (25  $\mu$ M), BAY87 (10  $\mu$ M), or DMSO and TGEV (multiplicity of infection [MOI]=1) for 1 h at 4  $^{\circ}$ C. After washing with PBS, TGEV N mRNA levels were measured by RT-qPCR. (B) Penetration assay. ST cells (left) or the intestinal organoid monolayer (right) were infected with TGEV (MOI=1) for 1 h at 4  $^{\circ}$ C and then treated with CoCl<sub>2</sub> (25  $\mu$ M), BAY87 (10  $\mu$ M), or DMSO for 2 h at 37  $^{\circ}$ C after washing with PBS. Cell samples were washed using sodium citrate buffer and examined using RT-qPCR. (C) Replication assay. ST cells (left) or the intestinal organoid monolayer (right) infected with TGEV (MOI=1) were incubated at 37  $^{\circ}$ C for 3 h and washed with sodium citrate buffer. The cells were then treated with CoCl<sub>2</sub> (25  $\mu$ M), BAY87 (10  $\mu$ M), or DMSO for 13 h. The cells were harvested and examined by RT-qPCR. (D) Release assay. ST cells (left) or the intestinal organoid monolayer (right) were infected with TGEV (MOI=1) for 16 h, and then CoCl<sub>2</sub> (25  $\mu$ M), BAY87 (10  $\mu$ M), or DMSO was added to the cells for 4 h. RT-PCR was used to test the viral load in the supernatant. Results are presented as the mean  $\pm$  standard deviation of data from three independent experiments \*\*\*,  $P \leq 0.001$ ; ns, not significant, determined by two-tailed Student's  $t$ -test.

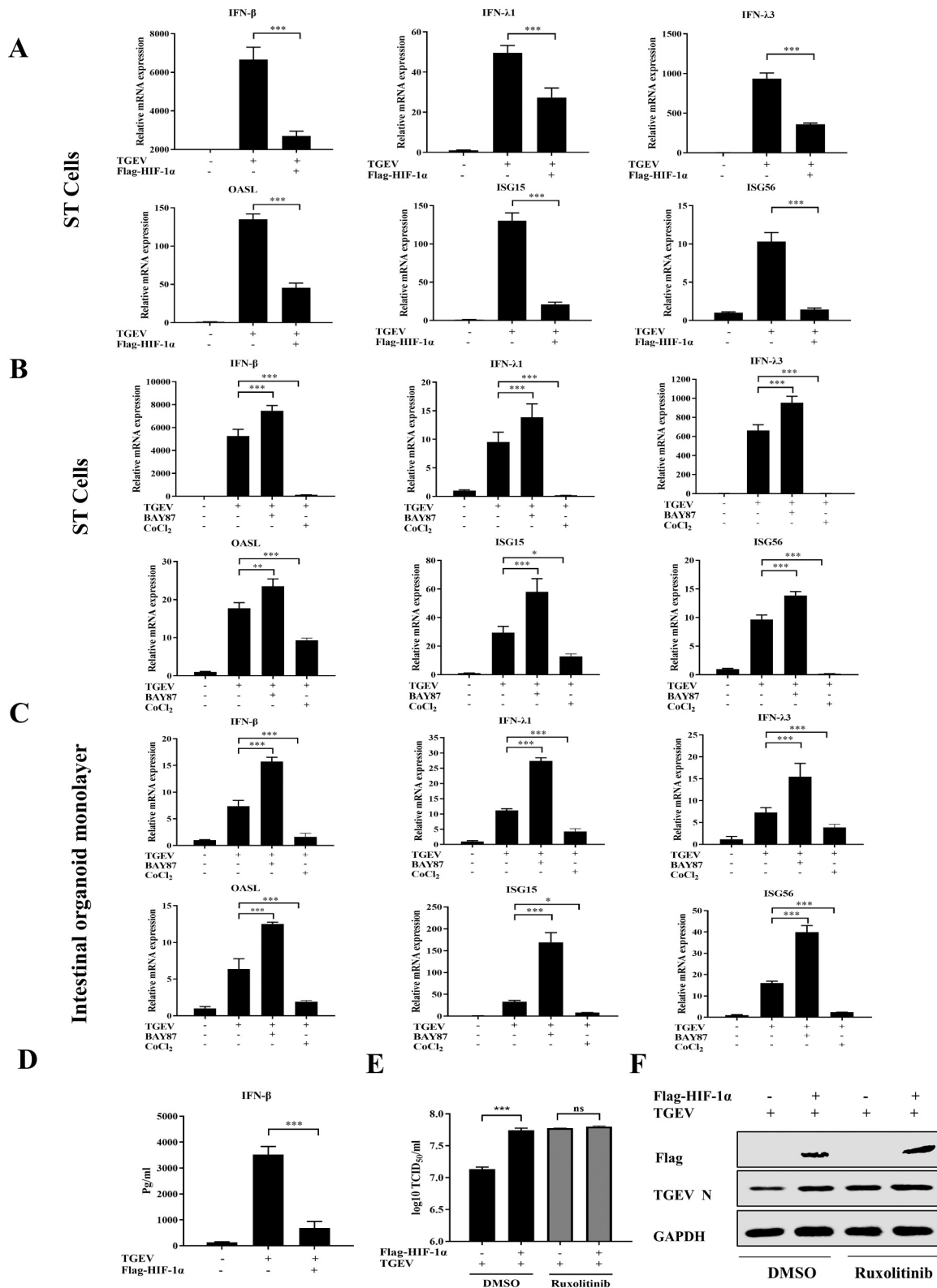


**Fig. 4.** HIF-1 $\alpha$  facilitates TGEV replication by downregulating type I and type III IFN production. (A) ST cells transfected with Flag-HIF-1 $\alpha$  for 24 h were infected with TGEV (multiplicity of infection [MOI]=1) for 20 h. Transcriptional levels of IFN- $\beta$ , IFN- $\lambda$ 1, IFN- $\lambda$ 3, OASL, ISG15, and ISG56 were evaluated by RT-qPCR. (B, C) ST cells (B) or the intestinal organoid monolayer (C) were treated with BAY87(10  $\mu$ M) or CoCl<sub>2</sub> (25  $\mu$ M) and infected with TGEV (MOI=1) for 20 h. Transcriptional levels of IFN- $\beta$ , IFN- $\lambda$ 1, IFN- $\lambda$ 3, OASL, ISG15, and ISG56 were detected by RT-qPCR. (D) ST cells transfected with Flag-HIF-1 $\alpha$  for 24 h were infected with TGEV (MOI=1) for 20 h. IFN- $\beta$  was measured in the supernatant by enzyme-linked immunosorbent assay. (E, F) ST cells were treated with ruxolitinib (4  $\mu$ M) and transfected with Flag-HIF-1 $\alpha$  for 24 h, and then infected with TGEV (MOI=1) for 20 h. HIF-1 $\alpha$  in the supernatant and cell samples was detected by 50% tissue culture infectious dose (TCID<sub>50</sub>) assay and western blotting. Results are presented as the mean  $\pm$  standard deviation of data from three independent experiments \*,  $P \leq 0.05$ ; \*\*,  $P \leq 0.01$ ; \*\*\*,  $P \leq 0.001$ ; ns, not significant, determined by two-tailed Student's  $t$ -test.

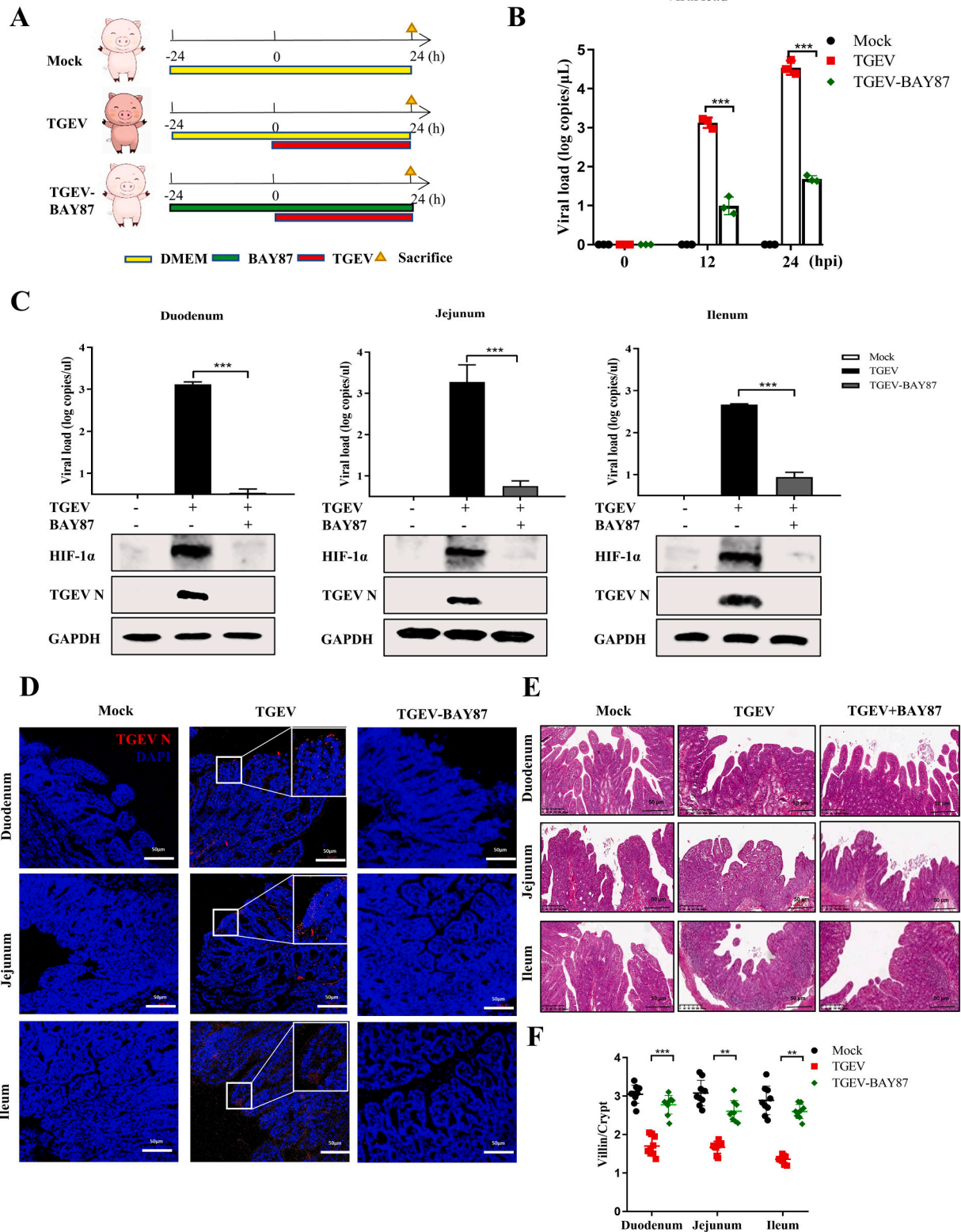


**Fig. 5. Pharmaceutical inhibition of HIF-1 $\alpha$  suppresses TGEV replication and pathogenesis *in vivo*.** (A) Experimental schemes for assessing the efficacy of BAY87 treatment against TGEV challenge in three groups of piglets. (B) Viral shedding was measured by RT-qPCR every 12 h post-infection (hpi). (C) TGEV genome copy numbers in the duodenum, jejunum, and ileum were detected by RT-qPCR, and HIF-1 $\alpha$  and TGEV N levels in the small intestine were determined by western blotting of samples from piglets sacrificed at 24 hpi. (D) Immunofluorescence analysis of TGEV N was conducted on different segments of the small intestine from piglets sacrificed at 24 hpi. Scale bar: 50  $\mu$ m. (E) Hematoxylin and eosin staining of three segments of the small intestine from piglets sacrificed at 24 hpi. Scale bar: 50  $\mu$ m. (F) Villin/crypt was calculated by Image J. Results are presented as the mean  $\pm$  standard deviation of data from three independent experiments \*\*,  $P \leq 0.01$ ; \*\*\*,  $P \leq 0.001$ , determined by two-tailed Student's *t*-test.

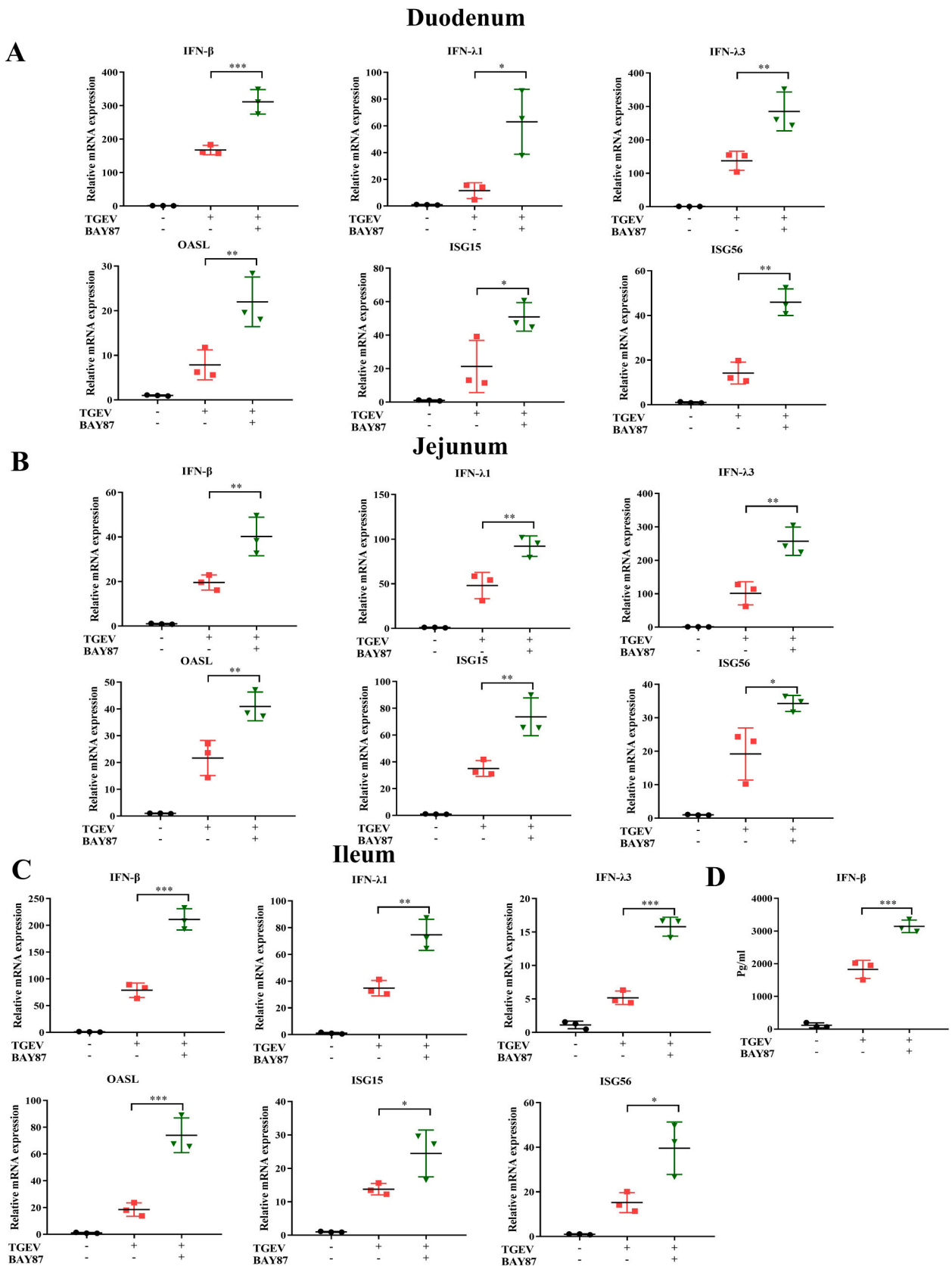


**Fig. 6.** Oral administration of the HIF-1 $\alpha$  inhibitor BAY87 induces an antiviral state in the piglet intestine by upregulating type I and type III IFN production. (A–C) Transcriptional levels of IFN- $\beta$ , IFN- $\lambda$ 1, IFN- $\lambda$ 3, OASL, ISG15, and ISG56 in the duodenum (A), jejunum (B), and ileum (C) of piglets sacrificed at 24 h post-infection (hpi) were detected by RT-qPCR. (D) IFN- $\beta$  levels in the intestinal digesta of piglets sacrificed at 24 hpi were measured by enzyme-linked immunosorbent assay. Results are presented as the mean  $\pm$  standard deviation of data from three independent experiments \*,  $P \leq 0.05$ ; \*\*,  $P \leq 0.01$ ; \*\*\*,  $P \leq 0.001$ , determined by two-tailed Student's  $t$ -test.



### 3. Results

#### 3.1. TGEV infection promotes HIF-1 $\alpha$ expression *in vitro* and *ex vivo*

TGEV infection can upregulate HIF-1 $\alpha$  expression in apical-out intestinal organoids at 48 hpi (unpublished data). To examine the response of HIF-1 $\alpha$  to TGEV infection in different cell models at various times, an intestinal organoid monolayer was established (Fig. S1A and B). ST cells and the intestinal organoid monolayer were infected with TGEV and the kinetics of HIF-1 $\alpha$  expression were assessed at different time points. TGEV infection was found to promote HIF-1 $\alpha$  protein and mRNA expression in ST cells and the intestinal organoid monolayer (Fig. 1A–D).

#### 3.2. HIF-1 $\alpha$ promotes TGEV infection in ST cells and the intestinal organoid monolayer

To further investigate the effect of HIF-1 $\alpha$  on TGEV infection, the HIF-1 $\alpha$  agonist CoCl<sub>2</sub> and HIF-1 $\alpha$  inhibitor BAY87 were employed. A cytotoxicity assay demonstrated that CoCl<sub>2</sub> at a concentration less than 50  $\mu$ M and BAY87 at a concentration less than 20  $\mu$ M had no effect on ST cells and intestinal organoid monolayer (Fig. S2A). Subsequently, ST cells and the intestinal organoid monolayer were treated with CoCl<sub>2</sub> for 1 h followed by infection with TGEV for 19 h. This CoCl<sub>2</sub> treatment induced HIF-1 $\alpha$  expression and led to an increase in TGEV infection (Fig. 2A and B). HIF-1 $\alpha$  overexpression was also shown by RT-qPCR, TCID<sub>50</sub>, and western blotting to enhance TGEV infection (Fig. 2C). In contrast, BAY87 downregulated HIF-1 $\alpha$  expression and inhibited TGEV infection in ST cells (Fig. 2D) and the intestinal organoid monolayer (Fig. 2E). These results indicated that HIF-1 $\alpha$  can promote TGEV infection in ST cells and the intestinal organoid monolayer.

#### 3.3. HIF-1 $\alpha$ enhances TGEV infection by targeting viral replication

A time-of-drug-addition assay was performed to determine which step of TGEV infection was affected by HIF-1 $\alpha$ . The impact of HIF-1 $\alpha$  on the adsorption, internalization, replication, and release of TGEV was evaluated in ST cells and the intestinal organoid monolayer. CoCl<sub>2</sub> and BAY87 treatment had no effect on virus adsorption, entry, or release (Fig. 3A, B, and D and Fig. S3A) but significantly affected TGEV replication (Fig. 3C and S4A). These findings suggested that HIF-1 $\alpha$  can upregulate TGEV infection by targeting viral replication.

#### 3.4. HIF-1 $\alpha$ facilitates TGEV replication by downregulating type I and type III IFN production

The mechanism by which HIF-1 $\alpha$  facilitates TGEV replication was explored by evaluating intrinsic antiviral defenses, including endoplasmic reticulum (ER) stress (glucose-regulated protein 78 [GRP78] and activating transcription factor 4 [ATF4]), autophagy (LC3B and autophagy-related 7 [ATG7]), apoptosis (caspase 3 and FasL), and IFN responses, after overexpressing HIF-1 $\alpha$  in TGEV-infected cells. HIF-1 $\alpha$  slightly regulated GRP78, ATF4, and caspase 3 expression, but significantly inhibited type I and type III IFN production (Fig. 4A and Fig. S5A). In addition, BAY87 treatment resulted in an obvious increase in TGEV-induced IFN and ISGs production, whereas CoCl<sub>2</sub> treatment significantly downregulated TGEV-induced IFN and ISGs production *in vitro* and *ex vivo* (Fig. 4B and C). ELISA results indicated a similar trend (Fig. 4D). To explore whether type I and type III IFN production correlated with HIF-1 $\alpha$ -induced TGEV infection, the cells were treated with ruxolitinib, which disrupts the IFN response by inhibiting Janus kinase 1 (JAK1) and Janus kinase 2 (JAK2). TGEV-induced IFN responses were significantly decreased by ruxolitinib treatment (Fig. S6A). Furthermore, HIF-1 $\alpha$  overexpression was unable to enhance TGEV infection after ruxolitinib treatment compared to DMSO treatment (Fig. 4E and F). Vero-APN cells, characterized by their deficiency in IFN responses, were

utilized to further investigate the correlation between IFN responses and the promotion of TGEV infection by HIF-1 $\alpha$ . The results confirm that HIF-1 $\alpha$  is unable to enhance TGEV replication under IFN-deficient conditions (Fig. S7A). Collectively, these findings illustrated that HIF-1 $\alpha$  enhanced TGEV replication by downregulating type I and type III IFN production.

#### 3.5. Pharmaceutical inhibition of HIF-1 $\alpha$ suppresses TGEV replication and pathogenesis *in vivo*

The *in vitro* and *ex vivo* results suggested that HIF-1 $\alpha$  could be a potential target for controlling TGEV infection in piglets. To explore this theory, the effect of HIF-1 $\alpha$  on TGEV infection was assessed in neonatal pigs *in vivo*. Piglets were treated with BAY87 or DMEM and individually inoculated with TGEV through oral administration (Fig. 5A). Anal swabs were collected every 12 h. Animals in the TGEV group exhibited higher viral shedding than those receiving BAY87 (Fig. 5B), and RT-qPCR and western blotting indicated that the TGEV burden and HIF-1 $\alpha$  expression in the small intestine were substantially lower in the BAY87-TGEV group than in the TEGV group (Fig. 5C). Immunofluorescence analysis showed that TGEV N protein production was almost entirely inhibited by BAY87 treatment (Fig. 5D). To further examine the effect of BAY87 on TGEV-induced damage to the small intestine, segments of the small intestine were paraffin-embedded, sliced, and stained with hematoxylin and eosin. BAY87 almost reversed the villous atrophy of small intestinal segments (Fig. 5E and F). Collectively, these data demonstrated that the inhibition of HIF-1 $\alpha$  by BAY87 treatment restricted TGEV replication and pathogenesis *in vivo*.

#### 3.6. Oral administration of the HIF-1 $\alpha$ inhibitor BAY87 induces an antiviral state in the piglet intestine by upregulating type I and type III IFN production

To confirm whether HIF-1 $\alpha$  could serve as a target for controlling TGEV infection, the mRNA expression levels of type I IFN, type III IFN, and ISGs were assessed in different segments of the small intestine. Oral administration of BAY87 to piglets upregulated IFN- $\beta$ , IFN- $\lambda$ 1, IFN- $\lambda$ 3, OASL, ISG15, and ISG56 in the duodenum (Fig. 6A), jejunum (Fig. 6B), and ileum (Fig. 6C). In addition, ELISA results demonstrated that pharmaceutical inhibition of HIF-1 $\alpha$  upregulated IFN- $\beta$  secretion in the intestinal digesta (Fig. 6D). These findings confirmed that the suppression of HIF-1 $\alpha$  by BAY87 strengthened the ability of the intestine to prevent TGEV replication *in vivo*.

## 4. Discussion

The ability of viruses to manipulate host factors is a vital immune evasion strategy that aids viral replication (Bouhaddou et al., 2023). For example, many viruses hijack HIF-1 $\alpha$  to promote infection. SARS-CoV-2 open reading frame 3a (ORF3a) induces HIF-1 $\alpha$  expression (Tian et al., 2021), whereas PRRSV nsp1 $\beta$  stabilizes HIF-1 $\alpha$  to enhance viral replication (Pang et al., 2022). This study found that TGEV infection significantly promoted HIF-1 $\alpha$  expression at different times in ST cells, the intestinal organoid monolayer, and *in vivo*, suggesting that this transcription factor participates in regulating TGEV infection.

HIF-1 $\alpha$  expression can be induced by an optimal concentration of CoCl<sub>2</sub> and is repressed by the appropriate concentration of BAY87 (Chang et al., 2023; Yue et al., 2023). Consequently, several researchers have used these two chemical compounds to regulate HIF-1 $\alpha$  expression. This study found that CoCl<sub>2</sub> treatment of ST cells and the intestinal organoid monolayer induced HIF-1 $\alpha$  and enhanced TGEV infection. In contrast, BAY87 treatment markedly reduced HIF-1 $\alpha$  expression and TGEV infection *in vitro* and *ex vivo*. HIF-1 $\alpha$  overexpression showed a similar trend. Although organoids are considered a physiological model for mimicking the intestinal microenvironment, animal experiments remain the most ideal model for exploiting the function of genes or

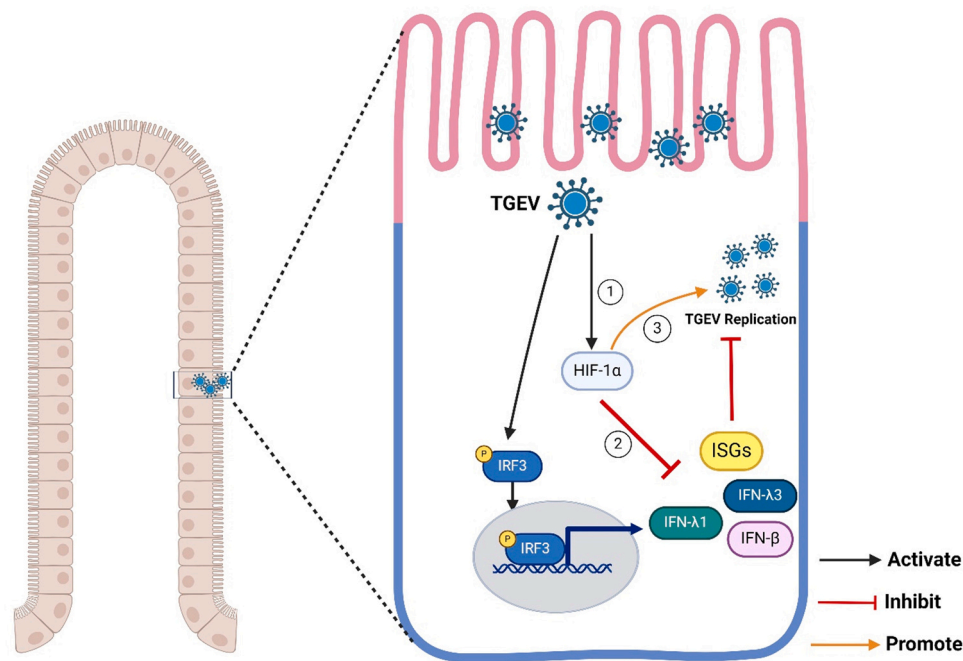


**Fig. 7. Proposed model of HIF-1 $\alpha$  facilitating TGEV replication by restraining type I and type III IFN production.** Step ①, TGEV infection upregulates HIF-1 $\alpha$  expression. Step ②-③, HIF-1 $\alpha$  inhibits type I and type III IFN production to promote TGEV replication. The diagram was created in BioRender.com.

drugs. In this study, experiments in piglets revealed that pharmaceutical inhibition of HIF-1 $\alpha$  suppressed TGEV replication and pathogenesis, suggesting that HIF-1 $\alpha$  could be a potential anti-TGEV target for the treatment of TGEV infection.

ER stress, autophagy, apoptosis, and IFN production are the primary intrinsic immune responses responsible for inhibiting virus replication (Majdoul and Compton, 2022). In this study, HIF-1 $\alpha$  facilitated TGEV infection by specifically targeting viral replication, not viral attachment, entry, or release. This finding suggests that HIF-1 $\alpha$  may impact TGEV replication by regulating ER stress, autophagy, apoptosis, and IFN responses. Subsequent analyses demonstrated that pharmaceutical upregulation or eukaryotic overexpression of HIF-1 $\alpha$  significantly restricted IFN- $\beta$ , IFN- $\lambda$ 1, IFN- $\lambda$ 3, OASL, ISG15, and ISG56 production *in vitro* and *ex vivo*. In addition, pharmaceutical inhibition of HIF-1 $\alpha$  upregulated the production of these cytokines *in vitro*, *ex vivo*, and *in vivo*. Several studies have shown that IFN- $\beta$ , IFN- $\lambda$ 1, IFN- $\lambda$ 3, OASL, and ISG15 have obvious antiviral effects on coronavirus replication (Ding et al., 2018; Park and Iwasaki, 2020; Song et al., 2022; Zhang et al., 2018), explaining how HIF-1 $\alpha$  can negatively regulate IFN responses to promote TGEV infection. ST cells (an immortal cell line), the intestinal organoids, and piglet intestine samples all showed the same trend throughout this study. A possible explanation for the congruent results despite organoids being a more physiological model than cell lines is that HIF-1 $\alpha$  is a high-expressed gene to promote TGEV replication by restraining IFN responses in different models or tissues. It is reported that HIF-1 $\alpha$  is also a transcriptional repressor of IRF5 and IRF3, which are transcription factors required for IFN responses in human monocytes (Peng et al., 2021). This may be the molecular mechanism by which HIF-1 $\alpha$  down-regulates IFN responses in porcine cell models, although further research is required to confirm this mechanism.

In conclusion, this study is the first to illustrate that HIF-1 $\alpha$  enhances TGEV infection by restraining type I and type III IFN responses in ST cells, the intestinal organoid monolayer, and in piglets (Fig. 7). The findings provide novel insight into the use of HIF-1 $\alpha$  as a potential therapeutic target for controlling TGEV infection.

## 5. Limitations of this study

Firstly, our study demonstrated that TGEV infection induces HIF-1 $\alpha$  expression *in vitro*, *ex vivo*, and *in vivo*. However, the mechanism by which TGEV prevents HIF-1 $\alpha$  degradation requires further exploration as a new research project. Additionally, we have validated that HIF-1 $\alpha$  facilitates TGEV replication by suppressing the production of type I and type III interferons. Notably, we have not investigated whether HIF-1 $\alpha$  regulates other porcine coronaviruses through a similar mechanism. This warrants further investigation to augment our understanding of the role of HIF in the prevention and control of porcine coronaviruses. Lastly, while HIF-1 $\alpha$  has been identified as a negative regulator of TGEV-induced interferon responses in cell models and piglets, the specific underlying mechanism of this phenomenon remains unclear. Further in-depth studies are needed to elucidate this aspect.

## CRediT authorship contribution statement

**Yue Zhang:** Data curation, Investigation. **Yifei Cai:** Validation. **Chen Tan:** Validation. **Ning Yang:** Data curation, Validation. **Yuan-yuan Liu:** Investigation. **Yuguang Fu:** Project administration. **Guan-guang Liu:** Conceptualization, Formal analysis, Funding acquisition, Supervision, Writing – review & editing. **Yunhang Zhang:** Formal analysis, Investigation, Methodology, Validation, Visualization, Writing – original draft. **Xue Rui:** Investigation. **Yang Li:** Data curation, Investigation.

## Declaration of Competing Interest

The authors declare that they have no known competing financial interests or personal relationships that could have appeared to influence the work reported in this paper.

## Acknowledgments

The authors thank Prof. Li Feng from Harbin Veterinary Research Institute, Chinese Academy of Agricultural Sciences, for providing a TGEV monoclonal antibody. We sincerely thank Dr. Jianing Chen for

technical support and acknowledge all group members of the Animal Immunology Group of Lanzhou Veterinary Research Institute for helpful discussions, animal care and breeding. This work was supported by the National Natural Science Foundation of China (U22A20522, 31972689), Natural Science Foundation of Technology Department, Gansu Province, China (20JR10RA020), CAAS International Exchange Scholarship for graduate students, the Science and Technology Major Project of Gansu Province (22ZD6NA001), and ULG-CAAS joint Ph.D. Program and CSC-WBI joint Ph.D. Program.

#### Authors' contributions

G.L. conceived the project. Y.Z., X.R., Y.L., Y.Z., Y.C., C.T., N.Y. and Y.L. performed the experiments. Y.Z., and G.L. analyzed the data. Y.Z. drafted the manuscript. G.L. and Y.F. edited the manuscript.

#### Appendix A. Supporting information

Supplementary data associated with this article can be found in the online version at [doi:10.1016/j.vetmic.2024.110055](https://doi.org/10.1016/j.vetmic.2024.110055).

#### References

- Bouhaddou, M., Reuschl, A.K., Polacco, B.J., Thorne, L.G., Ummadi, M.R., Ye, C., Rosales, R., Pelin, A., Batra, J., Jang, G.M., Xu, J., Moen, J.M., Richards, A.L., Zhou, Y., Harjai, B., Stevenson, E., Rojc, A., Ragazzini, R., Whelan, M.V.X., Furnon, W., De Lorenzo, G., Cowton, V., Syed, A.M., Ciling, A., Deutsch, N., Pirak, D., Dowgier, G., Mesner, D., Turner, J.L., McGovern, B.L., Rodriguez, M.L., Leiva-Rebollo, R., Dunham, A.S., Zhong, X., Eckhardt, M., Fossati, A., Liotta, N.F., Kehrer, T., Cupic, A., Rutkowska, M., Mena, I., Aslam, S., Hoffert, A., Foussard, H., Olwal, C.O., Huang, W., Zwaka, T., Pham, J., Lyons, M., Donohue, L., Griffin, A., Nugent, R., Holden, K., Deans, R., Aviles, P., Lopez-Martin, J.A., Jimeno, J.M., Obernier, K., Fabius, J.M., Soucheray, M., Huttenhain, R., Jungreis, I., Kellis, M., Echeverria, I., Verba, K., Bonfanti, P., Beltrao, P., Sharan, R., Doudna, J.A., Martinez-Sobrido, L., Patel, A.H., Palmarini, M., Miorin, L., White, K., Swaney, D.L., Garcia-Sastre, A., Jolly, C., Zuliani-Alvarez, L., Towers, G.J., Krogan, N.J., 2023. SARS-CoV-2 variants evolve convergent strategies to remodel the host response. *In: Cell*, 186, pp. 4597–4614 e4526.
- Chang, H.A., Ou Yang, R.Z., Su, J.M., Nguyen, T.M.H., Sung, J.M., Tang, M.J., Chiu, W. T., 2023. YAP nuclear translocation induced by HIF-1 $\alpha$  prevents DNA damage under hypoxic conditions. *Cell Death Discov.* 9, 385.
- Chen, Y., Zhang, Y., Wang, X., Zhou, J., Ma, L., Li, J., Yang, L., Ouyang, H., Yuan, H., Pang, D., 2023. Transmissible Gastroenteritis Virus: An Update Review and Perspective. *Viruses* 15.
- Ding, L., Li, J., Li, W., Fang, Z., Li, N., Guo, Q., Qu, H., Feng, D., Li, J., Hong, M., 2018. p53 mediated IFN- $\beta$  signaling to affect viral replication upon TGEV infection. *Vet. Microbiol.* 227, 61–68.
- Huang, X., Chen, J., Yao, G., Guo, Q., Wang, J., Liu, G., 2019. A TaqMan-probe-based multiplex real-time RT-qPCR for simultaneous detection of porcine enteric coronaviruses. *Appl. Microbiol. Biotechnol.* 103, 4943–4952.
- Koyasu, S., Kobayashi, M., Goto, Y., Hiraoka, M., Harada, H., 2018. Regulatory mechanisms of hypoxia-inducible factor 1 activity: Two decades of knowledge. *Cancer Sci.* 109, 560–571.
- Li, Y., Yang, N., Chen, J., Huang, X., Zhang, N., Yang, S., Liu, G., Liu, G., 2020. Next-generation porcine intestinal organoids: an apical-out organoid model for swine enteric virus infection and immune response investigations. *J. Virol.* 94, e01006–20.
- Liu, G., Lee, J.H., Parker, Z.M., Acharya, D., Chiang, J.J., van Gent, M., Riedl, W., Davis-Gardner, M.E., Wies, E., Chiang, C., Gack, M.U., 2021. ISG15-dependent activation of the sensor MDA5 is antagonized by the SARS-CoV-2 papain-like protease to evade host innate immunity. *Nat. Microbiol.* 6, 467–478.
- Liu, Q., Wang, H.Y., 2021. Porcine enteric coronaviruses: an updated overview of the pathogenesis, prevalence, and diagnosis. *Vet. Res. Commun.* 45, 75–86.
- Majdoul, S., Compton, A.A., 2022. Lessons in self-defence: inhibition of virus entry by intrinsic immunity. *Nat. Rev. Immunol.* 22, 339–352.
- Meng, X., Zhu, Y., Yang, W., Zhang, J., Jin, W., Tian, R., Yang, Z., Wang, R., 2023. HIF-1 $\alpha$  promotes virus replication and cytokine storm in H1N1 virus-induced severe pneumonia through cellular metabolic reprogramming. *Virol. Sin.*
- Pang, Y., Zhou, Y., Wang, Y., Sun, Z., Liu, J., Li, C., Xiao, S., Fang, L., 2022. Porcine reproductive and respiratory syndrome virus nsp1 $\beta$  stabilizes HIF-1 $\alpha$  to enhance viral replication. *Microbiol. Spectr.* 10, e0317322.
- Park, A., Iwasaki, A., 2020. Type I and type III interferons - induction, signaling, evasion, and application to combat COVID-19. *Cell Host Microbe* 27, 870–878.
- Peng, T., Du, S.Y., Son, M., Diamond, B., 2021. HIF-1 $\alpha$  is a negative regulator of interferon regulatory factors: Implications for interferon production by hypoxic monocytes. *Proc. Natl. Acad. Sci. USA* 118.
- Schneider, W.M., Chevillotte, M.D., Rice, C.M., 2014. Interferon-stimulated genes: a complex web of host defenses. *Annu. Rev. Immunol.* 32, 513–545.
- Shin, D., Mukherjee, R., Grewe, D., Bojkova, D., Baek, K., Bhattacharya, A., Schulz, L., Widera, M., Mehdipour, A.R., Tascher, G., Geurink, P.P., Wilhelm, A., van der Heden van Noort, G.J., Ovaa, H., Muller, S., Knobloch, K.P., Rajalingam, K., Schulman, B. A., Cinatl, J., Hummer, G., Ciesek, S., Dikic, I., 2020. Papain-like protease regulates SARS-CoV-2 viral spread and innate immunity. *Nature* 587, 657–662.
- Song, L., Chen, J., Hao, P., Jiang, Y., Xu, W., Li, L., Chen, S., Gao, Z., Jin, N., Ren, L., Li, C., 2022. Differential transcriptomics analysis of IPEC-J2 cells single or coinfecting with porcine epidemic diarrhea virus and transmissible gastroenteritis virus. *Front. Immunol.* 13, 844657.
- Tian, D., Mukherjee, R., Grewe, D., Bojkova, D., Baek, K., Bhattacharya, A., Schulz, L., Yue, M., Pan, P., Wang, W., Li, Y., Chen, X., Wu, K., Luo, Z., Zhang, Q., Wu, J., 2021. HIF-1 $\alpha$  promotes SARS-CoV-2 infection and aggravates inflammatory responses to COVID-19. *Signal Transduct. Target Ther.* 6, 308.
- Yang, N., Zhang, Y., Fu, Y., Li, Y., Yang, S., Chen, J., Liu, G., 2022a. Transmissible Gastroenteritis Virus Infection Promotes the Self-Renewal of Porcine Intestinal Stem Cells via Wnt/ $\beta$ -Catenin Pathway. *J. Virol.* 96, e0096222.
- Yang, S., Yang, N., Huang, X., Li, Y., Liu, G., Jansen, C.A., Savelkoul, H.F.J., Liu, G., 2022b. Pigs' intestinal barrier function is more refined with aging. *Dev. Comp. Immunol.* 136, 104512.
- Yue, Y., Tang, Y., Huang, H., Zheng, D., Liu, C., Zhang, H., Liu, Y., Li, Y., Sun, X., Lu, L., 2023. VBP1 negatively regulates CHIP and selectively inhibits the activity of hypoxia-inducible factor (HIF)-1 $\alpha$  but not HIF-2 $\alpha$ . *J. Biol. Chem.* 299, 104829.
- Zhang, K., Lin, S., Li, J., Deng, S., Zhang, J., Wang, S., 2022. Modulation of innate antiviral immune response by porcine enteric coronavirus. *Front. Microbiol.* 13, 845137.
- Zhang, N., Shi, H., Yan, M., Liu, G., 2021. IFIT5 negatively regulates the type I IFN pathway by disrupting TBK1-IKKeppilon-IRF3 signalosome and degrading IRF3 and IKKeppilon. *J. Immunol.* 206, 2184–2197.
- Zhang, Q., Ke, H., Bliklager, A., Fujita, T., Yoo, D., 2018. Type III interferon restriction by porcine epidemic diarrhea virus and the role of viral protein nsp1 in IRF1 signaling. *J. Virol.* 92.
- Zhang, Y., Song, Z., Wang, M., Lan, M., Zhang, K., Jiang, P., Li, Y., Bai, J., Wang, X., 2019. Cholesterol 25-hydroxylase negatively regulates porcine intestinal coronavirus replication by the production of 25-hydroxycholesterol. *Vet. Microbiol.* 231, 129–138.